Imaging doxorubicin and polymer-drug conjugates of doxorubicin-induced cardiotoxicity with bispecific anti-myosin-anti-DTPA antibody and Tc-99m-labeled polymers

Rajiv Panwar, PhD,[a] Prashant Bhattarai, MS,[a] Vishwesh Patil, PhD,[a] Keyur Gada, PhD,[a] Stan Majewski, PhD,[b] and Ban An Khaw, PhD[a]

[a] Department of Pharmaceutical Sciences, Northeastern University, Boston, MA
[b] University of Virginia, Charlottesville, VA

Received Sep 20, 2017; accepted Nov 15, 2017
doi:10.1007/s12350-018-1190-2

Background. **Radiolabeled anti-myosin imaging is well-established for imaging doxorubicin-induced cardiotoxicity. However, to enable imaging of drug-induced cardiotoxicity in small experimental animals, pretargeting with bispecific anti-myosin-anti-DTPA-Fab-Fab' and targeting with high-specific radioactivity Tc-99m-DTPA-succinylated-polylysine (DSPL) was developed.**

Methods. **Mice were injected biweekly with 10 mg/kg Dox or its equivalent as D-Dox-PGA. Tc-99m-DSPL myocardial activity after pretargeting with bsAb-Fab-Fab' was determined after gamma imaging performed at day 7 for Dox-treated mice and day 39 for all others.**

Results. **Mice treated with 10 mg/kg Dox lost 10% total body weight in 1 week and 20% after a second dose. Pretargeted mice treated with 30 mg/kg cumulative D-Dox-PGA dose showed no loss of body weight for the duration of the study. Cardiotoxicity was confirmed by gamma imaging and scintillation counting (1.9 ± 0.25 [mean% ID/g ± SD]) after 1 dose of Dox. Mice injected with 3 × 10 mg/kg Dox equivalent as D-Dox-PGA (0.4 ± 0.04, $P < .01$) and untreated 2 control groups (0.20 ± 0.05 and 0.19 ± 0.04, $P < .01$) showed significantly lower myocardial anti-myosin radioactivity relative to the 10 mg/kg Dox group.**

Conclusion. **Pretargeting with bsAb-Fab-Fab' and targeting with Tc-99m labeled high-specific activity polymers enabled early visualization of doxorubicin induce cardiotoxicity in mice. Tolerated dose of D-Dox-PGA was greater than to 30 mg/kg Dox-equivalent dose with minimal cardiotoxicity. (J Nucl Cardiol 2019;26:1327–44.)**

Key Words: Doxorubicin cardiotoxicity • gamma imaging • pretargeting with bispecific antibody • polymer-drug conjugates

Electronic supplementary material The online version of this article (https://doi.org/10.1007/s12350-018-1190-2) contains supplementary material, which is available to authorized users.

The authors of this article have provided a PowerPoint file, available for download at SpringerLink, which summarises the contents of the paper and is free for re-use at meetings and presentations. Search for the article DOI on SpringerLink.com.

Funding This work was supported by an unrestricted grant of the corresponding author from Gwathmey Inc., LLC, Cambridge, MA.

Reprint requests: Ban An Khaw, PhD, Department of Pharmaceutical Sciences, Northeastern University, Boston, MA 02115; *b.khaw@northeastern.edu*

1071-3581/$34.00

Abbreviations	
Dox	Doxorubicin
DTPA	Diethylene triamine penta acetic acid
PGA	Polyglutamic acid
DSPL	DTPA-modified succinylated polylysine
D-Dox	DTPA and doxorubicin-conjugated
FITC	Fluorescein isothiocyanate
MTD	Maximum tolerated dose
MAb	Monoclonal antibody
bsAb	Bispecific antibody
TNBS	Trinitrobenzene sulfonic acid

See related editorial, pp. 1345–1347

INTRODUCTION

Anthracycline-induced cardiotoxicity is the major limitation of Dox for cancer therapy[1–5] possibly due to generation of reactive oxygen species.[6,7] Dexrazoxane, an iron chelator, ameliorated anthracycline-induced cardiotoxicity.[8,9] Topoisomerase 2β inhibition is also a mediator of anthracycline-induced cardiotoxicity.[10] However, detection of inhibition of Topoisomerase 2β cannot be used as a non-invasive method for diagnosis of impending cardiotoxicity. The gold standard for diagnosis of anthracycline-induced cardiotoxicity is endomyocardial biopsy[11]; however, it is not used routinely due to its invasiveness.[12] Non-invasive diagnostic methods such as equilibrium radionuclide angiocardiography, echocardiography, and magnetic resonance imaging can assess left ventricular function and pathology,[13] cardiac dysfunction,[14] or non-specific events, such as edema, inflammation, and fibrosis. Imaging of apoptosis in cardiomyopathy has also been used in experimental animals.[15]

Anti-myosin labeled with In-111 is a highly efficient non-invasive method for imaging Dox-induced cardiotoxicity[16–18] and other cardiomyopathies.[19] However, due to the diffused nature of the disease and low radiotracer accumulation, heart to lung ratios were needed for quantitation,[20] and most importantly, the unavailability of anti-myosin for clinical use[21] and the limitation on the ability to detect cardiotoxicity early justifies development of a new Tc-99m-based bispecific anti-myosin imaging approach utilizing the high specificity of anti-myosin and high-specific radioactivity radiolabeled polymers that can provide diagnostic images early after radiotracer administration, especially for small animal experimental studies.

Conjugation of chemotherapeutic drugs to polymers reduced non-target toxicity while increasing drug loading capacity and hydrophilicity of hydrophobic drugs.[22,23] The aim of our study is to demonstrate that pretargeting with bsAb-Fab-Fab' and targeting with Tc-99m-labeled DSPL can provide early diagnostic images of Dox-induced cardiotoxicity and attenuation of cardiotoxicity when D-Dox-PGA is substituted for Dox.

MATERIALS AND METHODS

Animals Male Balb/C mice (20-22 g) were used in our studies in accordance with the protocol # 11-0924R approved by the Institutional Animal Care and Use Committee of Northeastern University conforming to the NIH guidelines.

Cell lines Anti-DTPA-2C31E11C7 murine hybridoma (a subclone of 6C31H3),[24,25] anti-Myosin 2G42D7 murine hybridoma,[26] and rat embryonic cardiocyte H9c2 (ATCC) were grown in Dulbecco's Modified Eagle Medium (DMEM) supplemented with 10% Fetal clone, penicillin, streptomycin, and Amphotericin (2.5 μg/mL) at 37 °C in 5% CO_2.[24]

DTPA-Succinyl Fluorescein Polylysine Polymers (DS-F-PL)

Diethylene triamine penta acetic acid (DTPA, Sigma) was covalently conjugated to polylysine as described previously[24,25] with slight modification for labeling with Fluorescein Isothiocyanate (FITC) (Sigma Aldrich) (Supplemental Material). Modification of lysine residues with DTPA as well as FITC was assessed by the tri nitro benzene sulfonic acid (TNBS) assay.[27] FITC was conjugated to DTPA-polylysine and subsequent succinylation[24] are described in the Supplemental Material.

In Vitro Cell-Based Fluorescence Ligand Binding Assay

Epifluorescent microscopy was performed on Dox-treated H9c2 embryonic cardiocytes. H9c2 cells were seeded on microscope slides (Lab-Tek™ Chamber Slides) at 40,000 cells per chamber and the cells were allowed to grow until 80% confluent. Cells were treated with 10 μM Dox for 24 hours at 37 °C. Then, they were incubated with 1 μg/mL bsAb, 1 μg/mL FITC-labeled anti-myosin antibody or 1 μg/mL anti-myosin antibody for 1 hour. The cells were washed with cold 0.1 M PBS (3×) and those treated with bsAb were further incubated with DS-F-PL for 1 hour at 37°C. Cells treated with anti-myosin antibody were treated with FITC-labeled goat anti-mouse IgG antibody. After washing (3×), the cells were applied to microscope slides and cover slips were mounted using Fluoromount-G. The cells were examined with an epifluorescent microscope (Olympus DP70 and X-cite 120 Fluorescence 23 illumination system) using 34 ms exposure time to obtain digital micrographs. The images were processed using ImageJ software by NIH. Computerized planimetry was performed to determine the fluorescent intensity of each cell and the data presented as mean pixel intensity. The regions without cells were also computer planimetered to determine the background pixel intensity for normalization.

Antibodies

2G42D7 and 2C3E11C7 monoclonal antibodies (MAb) were purified from the ascitic fluid of mice immunized with 1.5 $\times$ 10^6 hybridomas of each cell line.[24,26] MAb were purified by Protein-G affinity chromatography and the purity was assessed by sodium dodecyl sulfate polyacrylamide gel electrophoresis (SDS-PAGE).[28] The immunoreactivity of pure MAb was assessed by ELISAs.[25]

Bispecific Anti-DTPA-Anti-myosin Antibody and Bispecific Anti-myosin-Anti-DTPA Fab-Fab' Antibody

bsAb were prepared as previously published[25] (Supplemental Material).

Anti-DTPA-Fab' was prepared by digestion of anti-DTPA MAb with immobilized pepsin-beads per instruction of the manufacturer (Pierce) and purification of $F(ab')_2$ fragments are described in the Supplemental material. Anti-DTPA $F(ab')_2$ was reduced with 10 mM dithiothreitol to generate Fab' fragments.[29,30] MAb anti-Myosin (2G42D7) Fab fragments were prepared by enzymatic digestion of intact monoclonal antibody with immobilized papain beads (Pierce)[26,28] (Supplemental Material).

Fab' of anti-DTPA antibody and the Fab of anti-myosin antibody were used to prepare the bsAb-Fab-Fab' complex (100 kDa) via thioether linkage[29,31] (Supplemental Material).

Purification of bsAb from Polymeric Bispecific and Unconjugated Antibodies

Intact bsAb anti-DTPA-Anti-myosin and bsAb anti-DTPA-Fab'-anti-myosin Fab were purified from free antibodies or fragments by HPLC size exclusion chromatography using a Zorbax GF-250 column (9.4 $\times$ 250 mm) (Agilent Technologies, separation range 10,000 to 400,000 Da) as previously reported[29,31] (Supplemental Material).

Immunoreactivity of the Intact bsAb and bsAb-Fab'-Fab

Enzyme-linked Immunosorbent assays. Immunoreactivities of the purified antibodies were assessed by standard ELISAs for anti-DTPA and anti-myosin antibodies as reported.[26]

ELISA for bispecific antibodies. Aliquots of 100 μL/well of Dog Heart Myosin (10 μg/mL) were loaded on 96-well micro-titer plates (BD Biosciences) and intact bsAb activity was assessed as previously described.[29,31] Data were analysed by GEN 5.0 software (Biotek Instruments Inc.).

Bispecific ELISA was performed as above to evaluate the immunoreactivities of bsAb-Fab-Fab'. DTPA-BSA and Dog Heart Myosin (DHM) were used as antigens to assess the immunoreactivities of anti-DTPA Fab' and anti-Myosin Fab, respectively.[29,31,32]

Preparation of Tc-99m-Labeled DSPL (14.6 kDa)

Diethylene triamine pentaacetic acid modified polylysine that was subsequently succinylated (DSPL) to render the nanopolymers negatively charged was prepared as previously described by Khaw et al.[24,31] The Zeta potential of DSPL was assessed using a Zeta Potential Analyzer; the Zeta Plus, (Brookhaven Instruments Corporation, Holtsville, NY).

Radiolabeling of DSPL was also as reported previously.[24,25,29,31] The radioactivity of each fraction was assessed using a dosimeter (Capentec Dose Calibrator).[28,31]

Preparation of D-Dox-PGA

Preparation of D-Dox-PGA was as previously published[31–33] (Supplemental Material).

Concentration of Dox in D-DOX-PGA was also assessed from 490 nm OD reading.[31–34] Presence of DTPA in D-Dox-PGA was demonstrated by ELISA.[31–33]

Determination of IC50 of Dox and D-Dox-PGA

Inhibitory concentration at 50% of cell viability (IC50) in Dox and D-Dox-PGA was determined in embryonic H9c2 cardiocytes as previously reported[33] at concentrations of 1, 2.5, 5, 10, 20, and 30 μg/mL of each drug. Formulae of correlation of cell viability to the drug concentrations were obtained by using the best fit curve program in Excel. The drug concentrations at 50% cell viability (IC50) were determined using these formulae.

In Vivo Animal Study Protocol

Balb/C mice (6-8 weeks old) (Charles River Laboratories, Wilmington, MA) were used in this study. All animals were given in food and water ad libitum.

Dox-Induced Cardiomyopathy in Balb/C Mice

Dox (10 mg/kg) or equivalent D-Dox-PGA was injected intravenously into Balb/c mice ($n = 5$ each group) biweekly or until the animal succumbed or day 39 was reached. Saline-injected mice and untreated mice were used as controls ($n = 5$). The schematic of the in vivo experimental protocol is shown in Figure 1A. The animals in the Dox treatment group that received two maximum tolerated doses (MTDs), died by day 20. Therefore, for in vivo and ex vivo comparison of cardiotoxicity induced by Dox to D-Dox-PGA, another group of mice ($n = 5$) was administered only 1 (10 mg/kg) MTD of Dox intravenously. In vivo imaging at day 8 was undertaken and compared with mice injected with 3 $\times$ 10 mg/kg MTD of D-Dox-PGA (equivalent to 4 $\times$ mean maximal tolerated dose of 7.5 mg/kg Dox) at day 39. All surviving mice were weighed daily for the duration of the study.

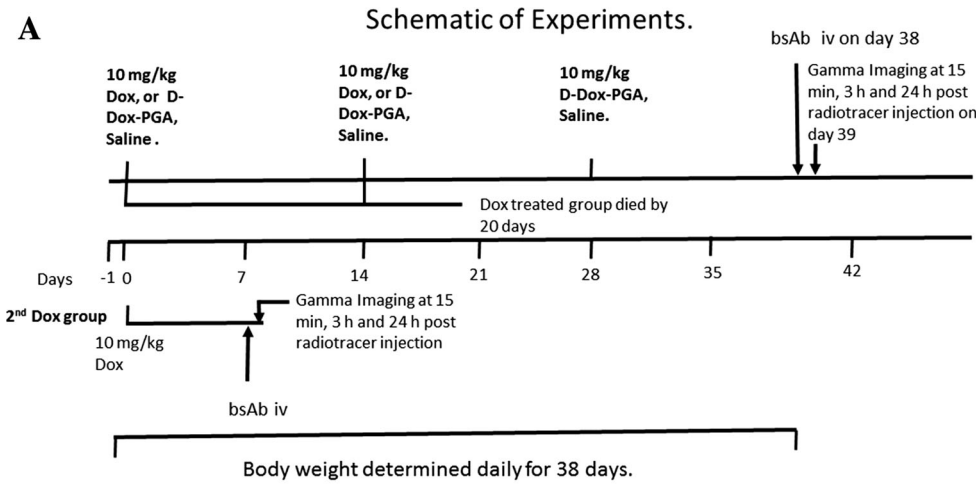
A
Schematic of Experiments.
10 mg/kg Dox, or D-Dox-PGA, Saline .
10 mg/kg Dox, or D-Dox-PGA, Saline.
10 mg/kg D-Dox-PGA, Saline.
bsAb iv on day 38
Gamma Imaging at 15 min, 3 h and 24 h post radiotracer injection on day 39
Dox treated group died by 20 days
Days -1 0 7 14 21 28 35 42
2nd Dox group
10 mg/kg Dox
Gamma Imaging at 15 min, 3 h and 24 h post radiotracer injection
bsAb iv
Body weight determined daily for 38 days.

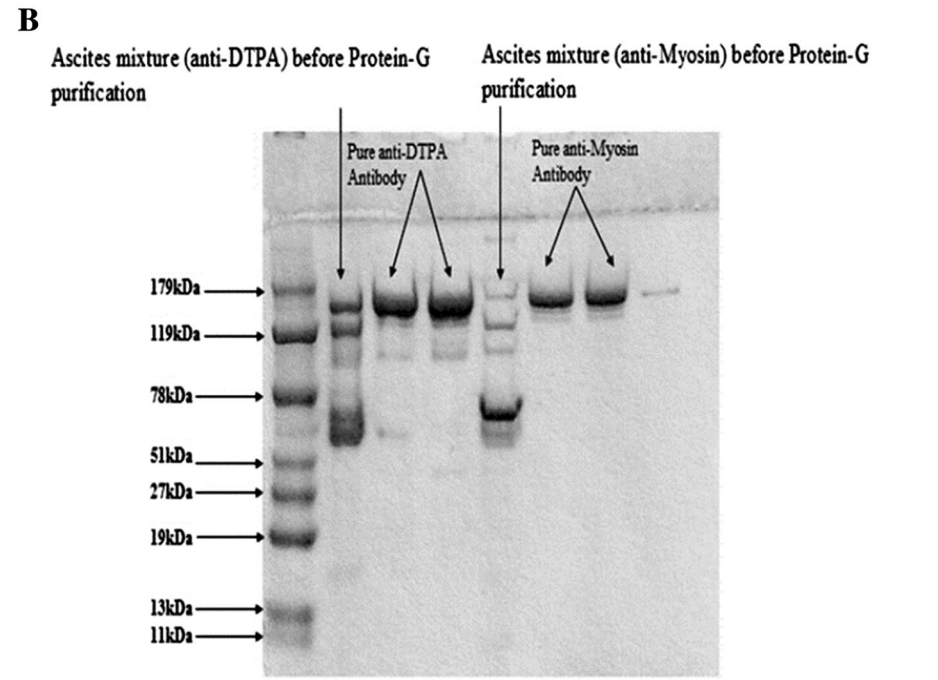
B
Ascites mixture (anti-DTPA) before Protein-G purification
Ascites mixture (anti-Myosin) before Protein-G purification
Pure anti-DTPA Antibody
Pure anti-Myosin Antibody
179kDa
119kDa
78kDa
51kDa
27kDa
19kDa
13kDa
11kDa

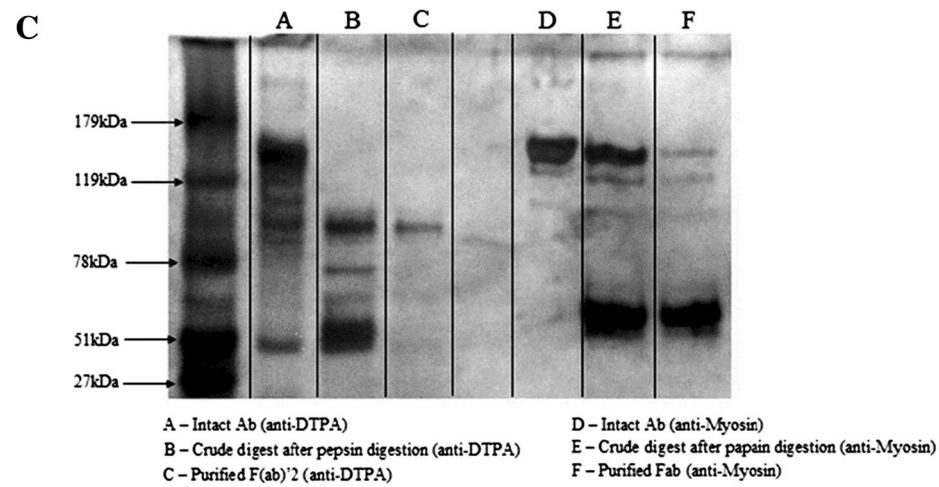
C
A B C D E F
179kDa
119kDa
78kDa
51kDa
27kDa
A – Intact Ab (anti-DTPA)
B – Crude digest after pepsin digestion (anti-DTPA)
C – Purified F(ab)'2 (anti-DTPA)
D – Intact Ab (anti-Myosin)
E – Crude digest after papain digestion (anti-Myosin)
F – Purified Fab (anti-Myosin)

◀ **Figure 1. A** The schematics of our in vivo experimental protocol. Total body weights were measured for each animal for free Dox-injected group, D-Dox-PGA injected, and Saline control group ($n = 5$ per group). The free Dox group was repeated ($n = 4$) for imaging of anti-myosin uptake after one 10 mg/kg dose of Dox at day 8. For the other two groups, D-Dox-PGA and Saline control groups, the bsAb was injected on the 38th day of the study and Tc-99m-DSPL was injected on the 39th day and gamma scintigraphic images were obtained at 15 minutes, 3 and 24-hour post-Tc-99m-DSPL intravenous administration. **B** SDS-PAGE of purified monoclonal anti-DTAP and anti-myosin antibodies and that of F(ab')$_2$ of anti-DTPA (Panel C [B and C]) and anti-myosin Fab [F].

In vivo imaging protocol. An aliquot of 10 μg of bsAb-Fab-Fab' was injected intravenously into each Balb/C mice ($n = 4$ or 5 mice per group). After approximately 18 hours, 37 MBq of Tc-99m DSPL was injected intravenously. Posteroanterior γ-images were acquired using a high resolution small animal gamma camera which was provided by the Jefferson National Accelerator Facility[35] as previously reported.[29,31] During each imaging session, a piece of filter paper (1 cm sq.) with 1.85 MBq radioactivity at the initiation of the imaging studies was included in the field of view as a standard. Image acquisition for planar gamma images was for 300 seconds at each time point (1×10^6 to 6×10^5 total counts). At 24 hours, a 30-minute acquisition time was employed to obtain at least 10,000 counts.[31] γ-images collected at 15 minutes, 3 and 24 hours were compared. Each control group received either bsAb-Fab-Fab' and Tc-99m DSPL, or just Tc-99m DSPL. Two mice from each group were randomly chosen and imaged, whereas all mice were injected with bsAb-Fab-Fab' and Tc-99m-DSPL including the placebo saline-injected group ($n = 5$) or just Tc-99m-DSPL in untreated (not handeled) group ($n = 4$) for biodistribution study. The daily body weight was not determined in the group of mice that were not handeled, whereas total body weight was measured in all other mice. The animals in the Dox treatment group were imaged at day 8, whereas animals receiving D-Dox-PGA and controls were imaged at day 39.

Biodistribution studies. After γ-imaging, all mice were sacrificed with intra-peritoneal over dose of ketamine (100 mg/kg) and xylazine (10 mg/kg). The heart, lung, liver, blood, kidney, spleen, stomach, intestine, muscle, salivary glands, and the injection site from each mouse were harvested and biodistribution was performed. All organs were weighed and radioactivity was assessed using a gamma scintillation counter (Compugamma model 1282—LKB Instruments, Inc.). Aliquots of 5 μL (1/10 the injected dose) of radiolabelled polymers were included for calculation of the total injected dose and tissue activity was presented as percent injected dose per gram (ID/gm). Radioisotope decay correction was applied to all sample counts.[28,32]

Histology. All hearts were collected after scintillation counting and were stored in OCT embedding medium at – 80 °C until processed. Ten micron sections of the frozen hearts were prepared using a Micron HM550 cryotome at – 20 °C as previously described.[32] The cryosections were then fixed on microscope slides and were examined for Dox fluorescence by epifluorescence microscopy.[31]

Statistical Analysis

Student's t test at 95% interval was used to assess statistical significance. A P value of $\leq .05$ was considered as statistically significant. One-way ANOVA was used to compare all myocardial Tc-99m activities pretargeted with bispecific anti-myosin-anti-DTPA antibodies or without pretargeting in 1 control group.

RESULTS

Anti-myosin and anti-DTPA MAb were assessed by SDS-PAGE to be greater than 90% pure (Figure 1B). F(ab')$_2$ and Fab were also demonstrated to be greater than 90% pure (Figure 1C).

The zeta potential of DSPL was determined to be -17.07 ± 2.59 and that of D-Dox-PGA was -21.57 ± 2.15. Both polymers had similar starting molecular weights of approximately 14.6 and 13.3 kDa and possess highly negatively charged zeta potentials.[31]

Figure 2A shows the HPLC elution profile of intact bsAb (top panel) and the corresponding bsAb activity (bottom panel). The right-most peak of the monomeric antibody shows no bsAb activity, whereas the middle and the left-most peaks showed bsAb activity. The corresponding SDS-PAGE of each fraction showed that fractions 15, 15.5, and 16 contained only dimeric bsAb, whereas fractions 12 to 14.5 contained mainly polymeric forms of the bsAb (Figure 2B).

Figure 3A shows the HPLC elution profile of the reaction mixture of bsAb-Fab-Fab' (top panel), the bsAb activity by ELISA of the corresponding fractions (bottom panel) and the SDS-PAGE of different HPLC fractions (Figure 3B). Only fraction 17.5 showed a peak with bsAb activity (Figure 3A, bottom panel) and the SDS-PAGE confirmed the presence of the dimeric bsAb-Fab-Fab' species with an approximate molecular weight of 100 kDa. This fraction was used subsequently for in vivo imaging studies.

Figure 4 shows the Sephadex G-25 column elution profile of D-Dox-PGA (solid circle) relative to that of free Dox (open circle). D-Dox-PGA eluted in the void

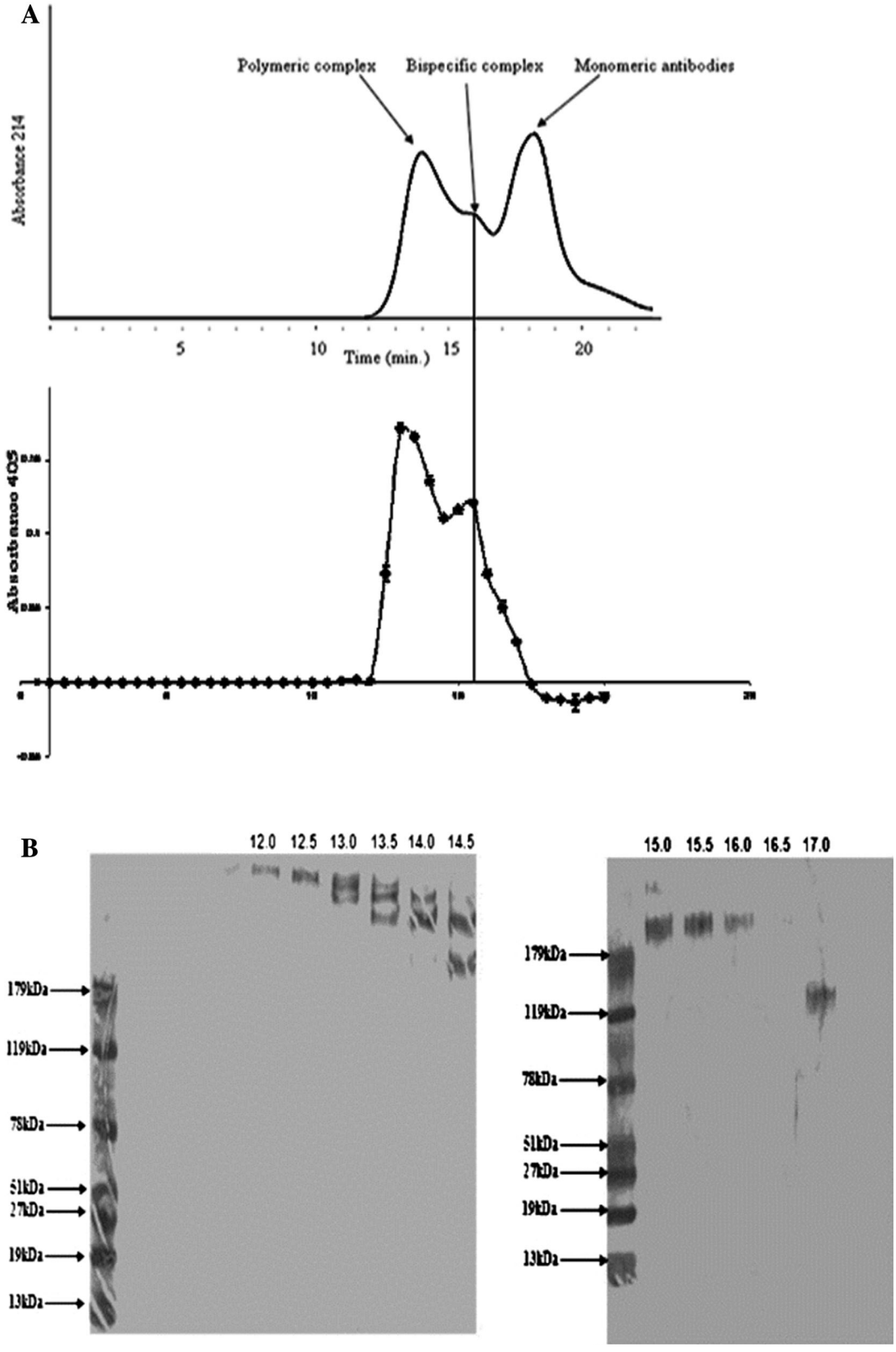
A
Polymeric complex
Bispecific complex
Monomeric antibodies
Absorbance 214
5
10
15
20
Time (min.)
B
12.0 12.5 13.0 13.5 14.0 14.5
15.0 15.5 16.0 16.5 17.0
179kDa
119kDa
78kDa
51kDa
27kDa
19kDa
13kDa

◀**Figure 2. A** HPLC elution profile of bsAB reaction mixture to separate bispecific antibody from monomeric antibodies (top panel) and the bsAb activity of the corresponding fraction of the elution profile (bottom panel). **B** SDS-PAGE of the HPLC chromatographic fractions showing fractions 15-16 containing bsAb with a molecular weight of 300 kDa. Fraction 17 contained monomeric unconjugated antibodies ($\simeq$ 150 kDa).

volume, whereas free Dox was eluted near or at the salt volume. The elution profile also demonstrated that all Dox used in the conjugation was conjugated to PGA.

Figure 5 shows the IC50 assessment for Dox and D-Dox-PGA in H9c2 embryonic cardiocytes. IC50 of D-Dox-PGA was 21.85 μg/mL Dox-equivalent concentration, whereas that of free Dox was 1.57 μg/mL. The exact IC50 values were calculated from the formulae of the two curves (open circles) $y = -0.116x^2 + 5.412x + 41.787$, $R^2 = 0.99$ for Dox and (closed circles) $y = -0.059x^2 + 3.946x - 8.059$, $R^2 = 0.97$) for D- = Dox-PGA. This resulted in a reduction of cardiocyte toxicity with D-Dox-PGA by approximately 14 times.

The ability of bsAb to target myosin in cell cultures is shown in Figure 6A where H9c2 cardiocytes treated with 10 μg/mL Dox for 24 hours were fixed to microscope slides and were treated with anti-myosin with secondary FITC-labeled goat anti-murine IgG antibody (G), anti-myosin-FITC (J), and bsAb and DS-F-PL (M). Red fluorescence of Dox is shown in B, E, H, K, and N and the corresponding phase contrast micrographs are shown in C, F, I, L, and O, respectively. The controls consisted of cell alone (A, B, and C) and those treated with DS-F-PL without pretargeting with bsAb (D, E, and F). The highest fluorescent intensity was obtained when treated cells were pretargeted with bsAb and targeted with DS-F-PL (Figure 6B).

Figure 7A shows the diagrammatic representation of the experiment protocol and a set of representative images obtained at 3 and 24-hour post-radiotracer injection and the % ID/g myocardial activity in three groups of mice. Figure 7B shows the whole-body serial planar gamma images of mice treated with Dox at 10 mg/kg MTD at day 8, D-Dox-PGA at 10 mg/kg × 3 doses, saline-injected control mice, pretargeted with bsAb-Fab-Fab' and targeted with Tc-99m-DSPL, and un-handeled control mice injected with Tc-99m-DSPL alone at day 39, after 15 minutes (left panels), 3 hours (middle panels), and 24 hours (right panels) post-administration of the radiotracer. Only the mouse treated with 1 dose of Dox showed myocardial activity at 3 and 24 hours (top middle and right panels). No myocardial activity was seen in the D-Dox-PGA-treated mouse at 3 × 10 mg/kg cumulative Dox-equivalent dose or in the control mice.

Figure 8A and B shows the 24 hours whole-body posteroanterior γ images of two sets of control mice (panels a and b), compared to D-Dox-PGA-treated mice (panels c) and Dox-treated mice (panels d). No myocardial activity was seen in the control animals. Both Dox-treated mice showed myocardial activity (Figure 8A and B, panels d). The image of the mouse in Figure 8A, panel d showed extensive myocardial activity. The second mouse (Figure 8B, panel d) showed less myocardial activity. Only 1 mouse treated with 30 mg/kg cumulative Dox-equivalent dose in the form of D-Dox-PGA showed minimal myocardial lesion activity indicative of some myocardial toxicity (arrow) (Figure 8A, panel c). The biodistribution data show (Figure 8C) that the radiotracer activity in hearts of mice with a single dose of Dox (10 mg/kg) lead to localization of 1.90 ± 0.04 % ID/g of Tc-99m-DSPL radioactivity, whereas radiotracer accumulation was statistically significantly lower (0.40 ± 0.04, $P > .001$) in the hearts of D-Dox-PGA-treated mice at a cumulative dose of 30 mg/kg at 39 days. The control untreated mice injected with bsAb-Fab-Fab' and targeted with Tc-99m DSPL or Tc-99m DSPL alone showed no myocardial activity in the gamma images (0.20 ± 0.05 and 0.19 ± 0.04 % ID/g, respectively) were also statistically significantly lower ($P < .001$, one-way ANOVA), but was not statistically different from the myocardial activity of mice injected with D-Dox-PGA (P = NS).

Determination of the total body weight of mice for the duration of the study, treated with Dox, D-Dox-PGA, and untreated controls are shown in Figure 9. In mice treated with one 10 mg/kg MTD of Dox, there was a mean total body weight loss of about 10% in 1 week. In the second group of mice treated with 2 × 10 mg/kg Dox, there was a mean loss of about 20% total body weight. In the group treated with D-Dox-PGA at 3 × 10 mg/kg Dox cumulative equivalent MTD, there was no loss of total body weight for the duration of the study. However, untreated controls gained weight.

Figure 10A shows the epifluoromicrographs of Dox fluorescence in the frozen myocardial tissue sections of

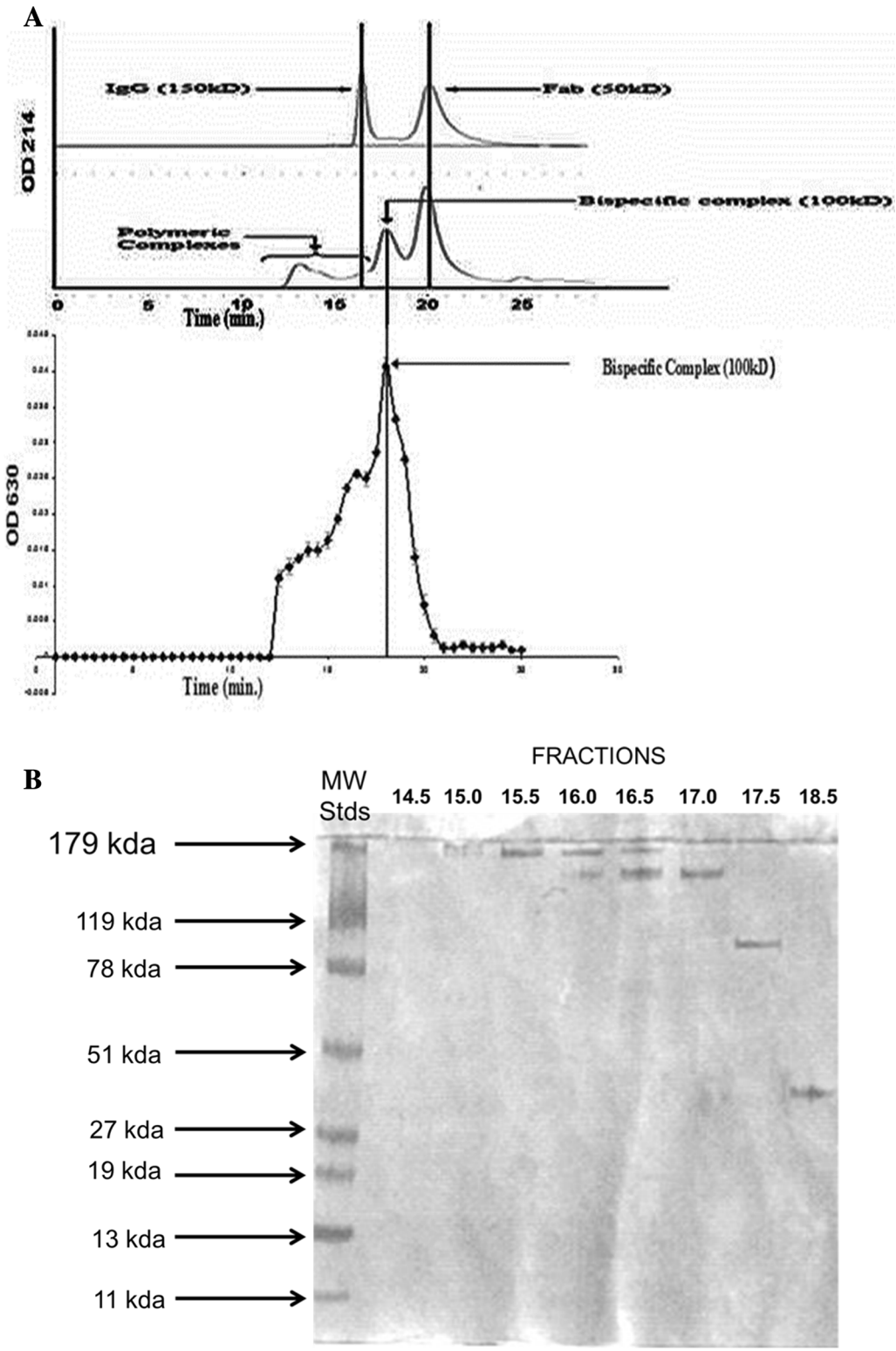

Figure 3. **A** HPLC elution profile of IgG and Fab and the reaction mixture of Fab'-Fab bispecific antibody preparation (top panel). The corresponding bispecific activity of the fractions show that the highest bispecific antibody activity corresponded to fraction 17.5 (bottom panel). **B** The corresponding SDS-PAGE of the fractions demonstrating that fraction 17.5 contained homogenous bsAb without free monomeric Fab or polymeric bsAbs.

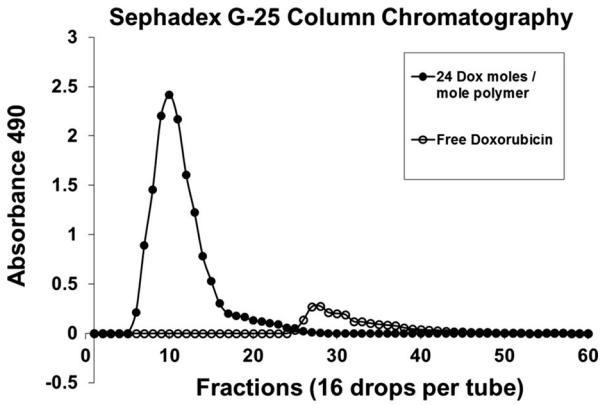

Figure 4. Elution profile of D-Dox-PGA relative to that of free Dox using a Sephadex G-25 size exclusion column. Closed circles = D-Dox-PGA, open circle = free Dox.

the groups described in the imaging and biodistribution studies. In this comparison, only one control group injected with bsAb-Fab-Fab' and Tc-99m DSPL was included since no Dox was administered to either of the control groups. Quantitative assessment of the mean fluorescent intensities is shown in Figure 10B. Only Dox-treated hearts showed significantly greater mean fluorescence intensity than hearts of mice treated with D-Dox-PGA or untreated controls ($P < .01$).

DISCUSSIONS

Our study showed that by using bispecific anti-myosin antibody complex that can target myosin specifically and at the same time enable capture of radiolabeled polymers with very high-specific radioactivity provided a new approach that allowed early diagnostic imaging of Dox-induced cardiotoxicity in very small murine hearts. Since the radiolabel is on a polymer, different radioisotopes may be substituted. In-111-labeled polymers have been used to image very small, sub-mm diameter prostate cancer lesion in the xenografted murine model.[29] If the chelator DTPA were substituted with deferroxamine, positron emitters, such as Ga-68, may be chelated on the polymers. Our approach is a versatile approach for in vivo antibody-targeted imaging. We have also demonstrated that the radioisotopes may be substituted with chemotherapeutic agents, such as Dox[31] and Paclitaxel.[36] Furthermore, the polymers are amenable for production of theranostic reagents where the polymers may carry both diagnostic and therapeutic agents simultaneously.

Dox is an effective and widely utilized anti-tumor drug for therapy of many types of cancers. Its optimal clinical use is limited by its cumulative dose-dependent cardiotoxicity.[37,38] Intercalation of DNA, production of

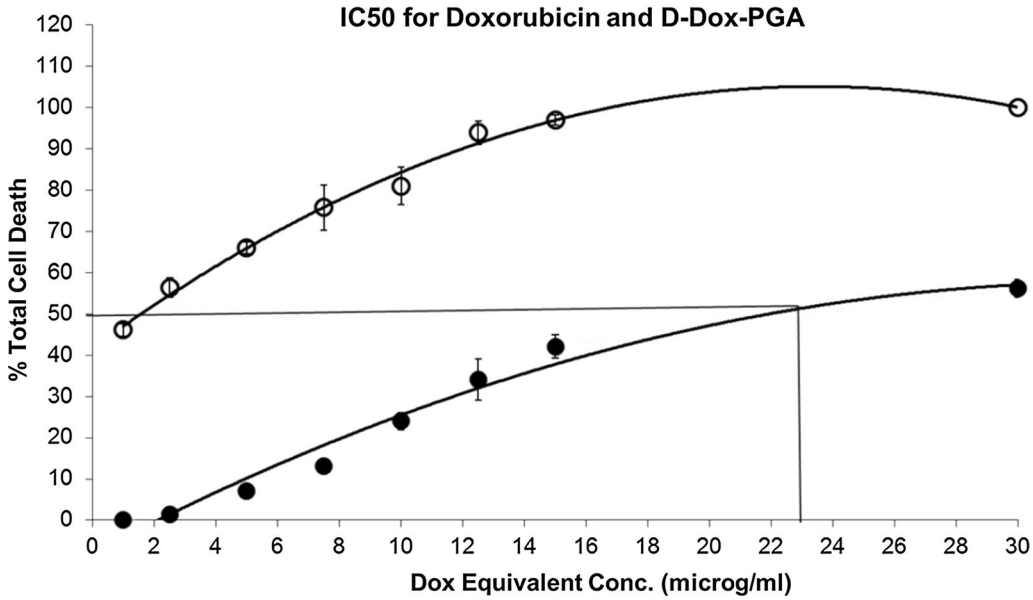

Figure 5. IC50 determination of Dox (open circles, $y = -0.116x^2 + 5.412x + 41.787$, $R^2 = 0.99$) and D-Dox-PGA (closed circles, $y = -0.059x^2 + 3.946x - 8.059$, $R^2 = 0.97$) in H9c2 rat embryonic cardiocytes in culture.

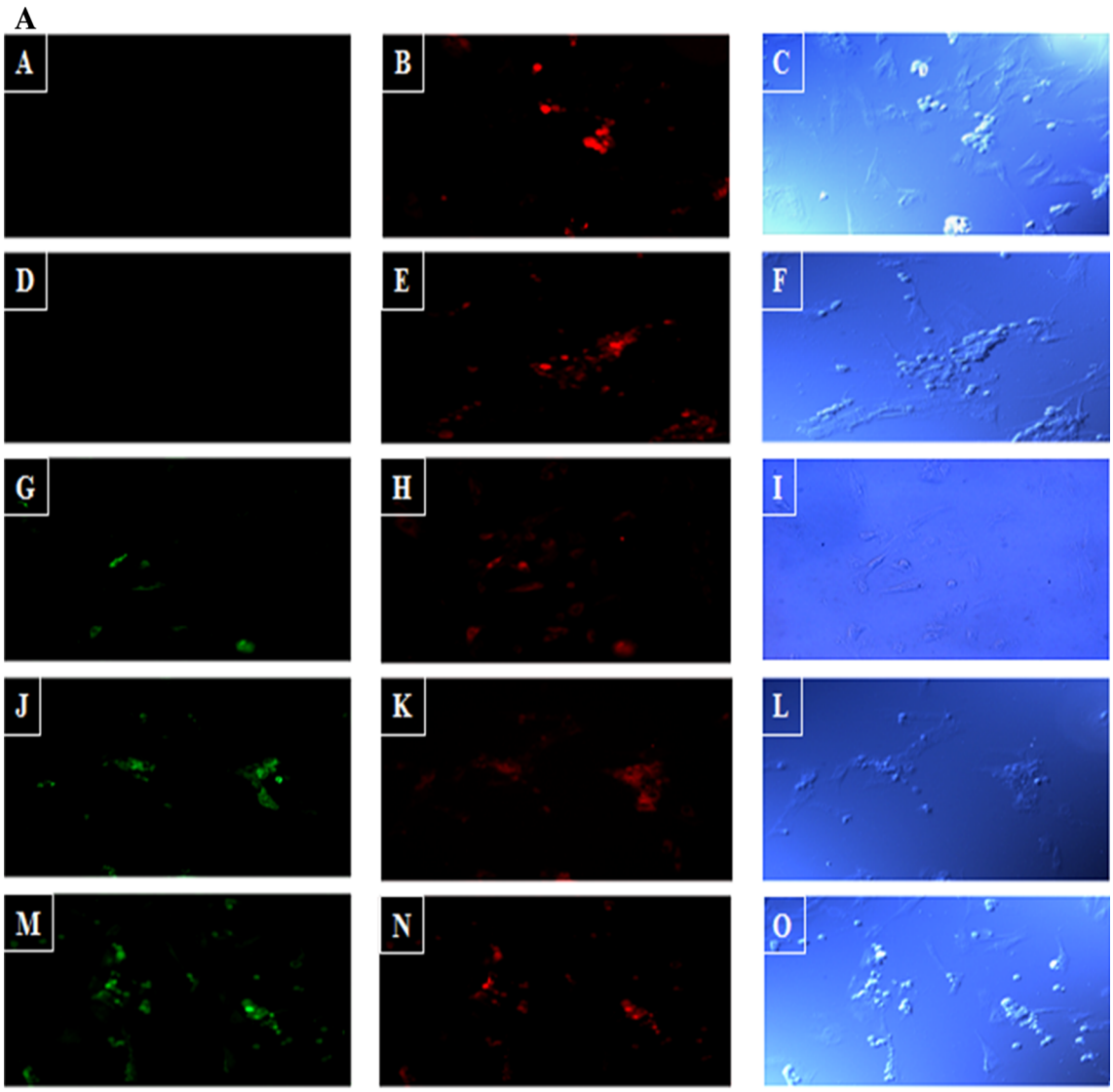
A
A
B
C
D
E
F
G
H
I
J
K
L
M
N
O
B
In-vitro Fluorescence
Adjusted mean intensity
8
7
6
5
4
3
2
1
0
1
0.1
0.01
0.001
0.0001
0.00001
Conc. (ug/ml)
BispAb+DS-F-PL
Anti-Myosin-FITC

◀ **Figure 6. A** Epifluoromicrograph showing targeting of H9c2 cardiocytes that had been treated with 10 mg/mL Dox for 24 hours, fixed to microscopic slides then treated with anti-myosin with secondary FITC-labeled goat anti-murine IgG antibody (G), anti-myosin FITC (J), and bispecific anti-DTPA-Anti-myosin antibody and DS-F-PL (M). Red fluorescence of Dox in the corresponding slides are shown in B, E, H, K, and N and the corresponding phase contrast micrographs in C, F, I, L, and O, respectively. The controls consist of cell alone (A, B, and C) and those treated with DS-F-PL without pretargeting with bsAb (D, E and F). **B** Computer planimetered fluorescent intensities of fluorescein of Dox-treated H9c2 cells as described in (**A**) stained with serial dilutions of bsAb (and DS-F-PL) or FITC-labeled anti-myosin antibody.

reactive oxygen species, inhibition of topoisomerase-2β,[10] extensive DNA damage, and initiation of apoptosis have been postulated as mechanisms of Dox-induced cardiotoxicity.[38] In a phase III clinical trial, the frequency of cardiotoxicity increased from 5% at a cumulative dose of 400 mg/m^2 to 48% at 700 mg/m^2.[38] Five percent of the cases of clinical heart failure and 5-20% of the cases with left ventricular dysfunction have been reported after Dox therapy.[39] Childhood cancer survivors who had received cumulative doses of Dox are eight times more likely to suffer severe cardiovascular diseases than the general population.[40] Therefore, various approaches, such as encapsulation of Dox, have been developed to reduce cardiotoxicity. Doxil and Myocet are 2 liposomal formulations. Encapsulated Dox maintained comparable anti-tumor properties, but both formulations have severe non-cardiac side effects, such as hand and foot syndrome,[41] follicular rashes, hyper-pigmentation, intertrigo-like eruption, and myelosuppression.[42,43] An FDA approved cardioprotective agent, dexrazoxane, an EDTA derivative that chelates iron, is used to reduce Dox cardiotoxicity[12] in extended treatment of metastatic breast cancer in women.[44] However, dexrazoxane also decreases the anti-tumor potency of Dox.[45,46] Similarly, Dox congeners have been employed to reduce cardiotoxicity. Nevertheless, hematological toxicity still remains.[47]

Although many novel Dox formulations have been tested in large clinical trials, many have failed to provide adequate comparable therapeutic efficacy and eliminate non-cardiotoxic effects. Therefore, there is still a need to develop novel and effective formulations of Dox which will not only have less non-target toxicity but also superior therapeutic potential. Also non-invasive or minimally invasive molecular imaging methods to assess cardiotoxicities associated with chemotherapy would be highly beneficial to cancer patients.

Anti-myosin antibody radiolabeled directly had been widely employed for diagnosis of various cardiomyopathies.[16–20,48] In-111-labeled anti-myosin was reported to be able to differentiate between doxorubicin and butylated hydroxyanisole protected doxorubicin-induced cardiotoxicities in a rat model.[49] However, this difference was assessable only by ex vivo scintillation counting of the hearts. Anti-myosin uptake ratio of 1.32:1 between rats treated with 10 mg/kg Dox and rats co-treated with 10 mg/kg Dox and 10 mg/kg butylated hydroxyanisole was significantly different ($P < .05$). Myocardial In-111 anti-myosin activity in untreated control rat hearts was 0.115 ± 0.013 % ID/g and in 30 mg/kg Dox-treated rat hearts was 0.203 ± 0.034 (3.74 Bq). In the current study, myocardial anti-myosin radioactivity of mice treated with 10 mg/kg Dox dose was approximately 0.703 MBq which is about 188 time more radioactivity per gram of the myocardium. Hiroe and co-workers also reported the ability to detect doxorubicin-induced cardiotoxicity in rats by In-111 anti-myosin localization. They obtained a higher ratio of 3.9 for the left ventricular activities between Dox treated and untreated control hearts.[50] Nevertheless, no in vivo images were provided. The macro- and micro-autoradiographs showed unequivocal anti-myosin localization in doxorubicin-induced cardiotoxic rat hearts. More recently, Su and co-workers were able to show by in vivo imaging using a PET tracer 18F-CP18, a caspase-3 substrate, the difference between Dox-induced cardiotoxicity and vehicle-treated mice.[51] The ratio from the microPET data was only 1.78:1 and that from autoradiography was 2.5:1. Hot spot localization of the 18F-CP18 in the 12-week treatment mouse was visible but there also appears to be substantial left ventricular blood activity in the region of the myocardium. No corresponding images of control mice were given. In our study, the ratio between Dox cardiotoxic- to normal-myocardium was 9.5:1 (Figure 8B). Therefore, at an ex vivo ratio of about 10:1 and an absolute radioactivity of about 0.703 MBq/g of the myocardium, in vivo imaging was readily obtained. Van Decker wrote in an article, ‘‘Imaging and chemotherapy cardiotoxicity: a long-playing story still seeking precision and improved outcome/management data,’’ pointing out the need for more precise and prognostic methods that may permit more effective intervention than assessment of the left ventricular function.[52] Positive anti-myosin localization has been reported to occur earlier than diagnosis of Dox

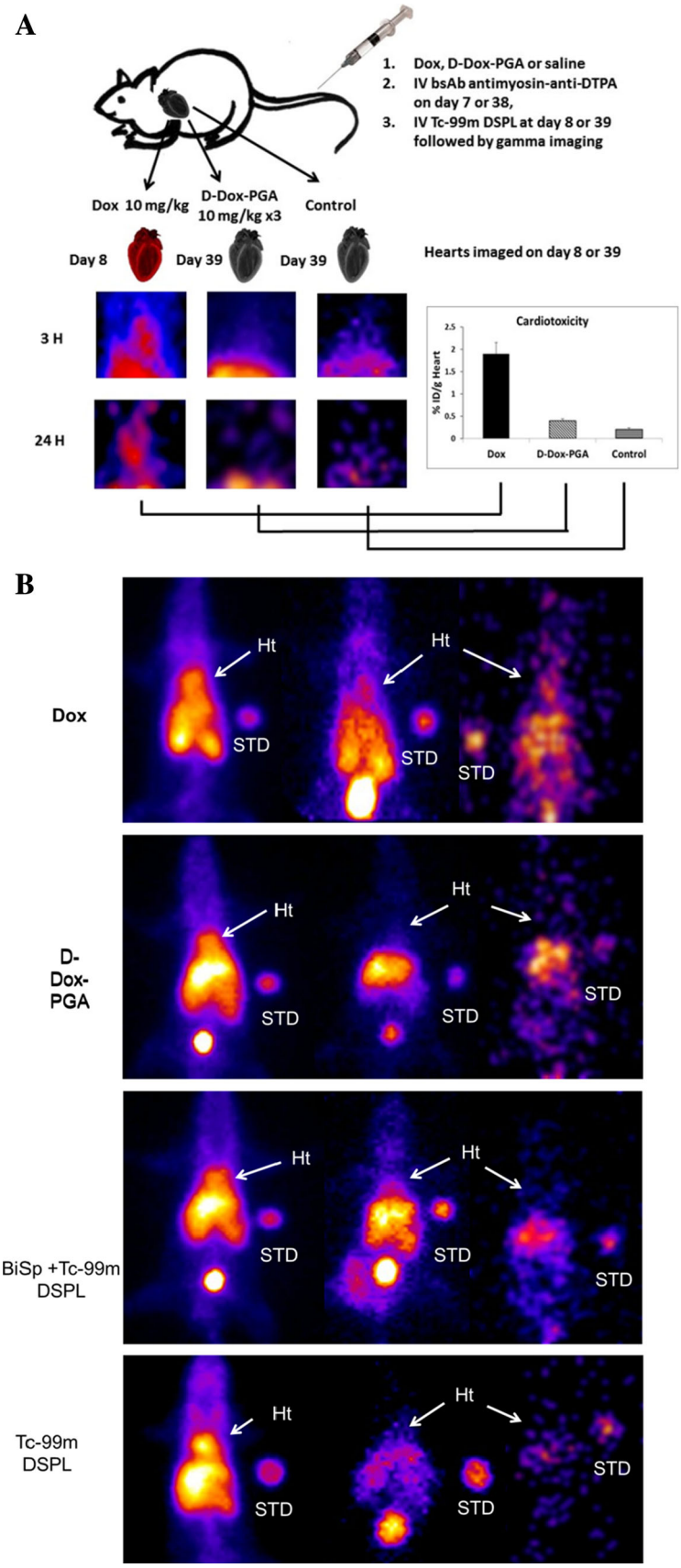
A
1. Dox, D-Dox-PGA or saline
2. IV bsAb antimyosin-anti-DTPA on day 7 or 38,
3. IV Tc-99m DSPL at day 8 or 39 followed by gamma imaging
Dox 10 mg/kg
D-Dox-PGA 10 mg/kg x3
Control
Day 8
Day 39
Day 39
Hearts imaged on day 8 or 39
3 H
24 H
Cardiotoxicity
% ID/g Heart
Dox
D-Dox-PGA
Control
B
Dox
D-Dox-PGA
BiSp +Tc-99m DSPL
Tc-99m DSPL
Ht
STD

◀ **Figure 7. A** Diagrammatic representation of the protocol used for gamma imaging of experimental mice (top panel) with representative close-up 3 and 24 hours images and the mean myocardial activity in % ID/g. **B** Shows whole-body antero-posterior serial gamma images of mice treated with 10 mg/kg free Dox at 15 minutes, 3 and 24 hours, (left, middle, and right panels, respectively) and 30 mg/kg cumulative Dox equivalent as D-Dox-PGA and untreated controls imaged after pretargeting with bsAb and targeting with Tc-99m DSPL, and control mice imaged with only Tc-99m DSPL (bottom panel). *Ht*, heart; *STD*, standard radioactivity on filter paper.

cardiotoxicity by conventional evidence.[17,53] Anti-myosin localization has been reported to occur earlier than significant deterioration of the LVEF.[54] However, In-111 anti-myosin is no longer available for clinical use.[21] Therefore, a Tc-99m version for myocardial imaging with anti-myosin would be highly desirable especially if this approach is as specific and more sensitive than In-111 anti-myosin Fab, and is also amenable to radiolabeling with PET radioisotopes such as Ga-68.

Our study reports a potential approach for improving diagnostic imaging of Dox-induced cardiotoxicity by the pretargeting and targeting approach. Two types of bsAb complexes were prepared for this study. A 300-kDa bsAb was used for proof of concept in vitro studies. A 100-kDa bsAb combining anti-DTPA-Fab' to anti-myosin Fab was prepared for in vivo imaging studies. The smaller bsAb unit allows blood clearance similar to that of $F(ab')_2$. We have used the overnight wait time of about 18 hours before administration of the radiolabeled polymers. Visualization of Dox-induced cardiotoxicity was feasible by 3-hour post-radiotracer injection (Figure 8). Myocardial radiotracer localization was confirmed by the follow-up 24-hour image of the same animal and by γ-scintillation counting of the excised heart. There was minimal or no myocardial activity in the D-Dox-PGA-treated mouse hearts and in the 2 control group hearts. The 24-hour images shown in Figure 9 reconfirm that this imaging approach can differentiate minimal myocardial injury between Dox, D-Dox-PGA, and non-Dox-treated controls in small murine hearts in vivo.

The limitation of the current report is that no immuno-histochemical studies of the myocardial tissues were performed to demonstrate localization of the bsAb. Nevertheless, epifluoromicrographs of the frozen heart sections treated with free Dox confirmed localization of Dox in the myocardium, whereas D-Dox-PGA had only background fluorescence (Figure 10A, B). Since anti-myosin has been amply reported to be highly specific and avid for targeting of irreversible myocardial injury, we did not repeat the immuno-histochemical demonstration with anti-myosin Fab, albeit in the bsAb format.

The current imaging studies also demonstrated that Dox cardiotoxicity may be reduced by conjugation of Dox to nanopolymers, such as PGA. Mean myocardial activity of D-Dox-PGA-treated mice (0.4 ± 0.04 % ID/g) was only 2 times that of the background activity of the controls (0.20 ± 0.04). Relative to uptake in the hearts treated with a single dose of free Dox (1.90 ± 0.25), D-Dox-PGA-treated hearts at 4 times the mean MDT had almost 5 times less myocardial injury. Our study did not achieve in determining the IC_{50}

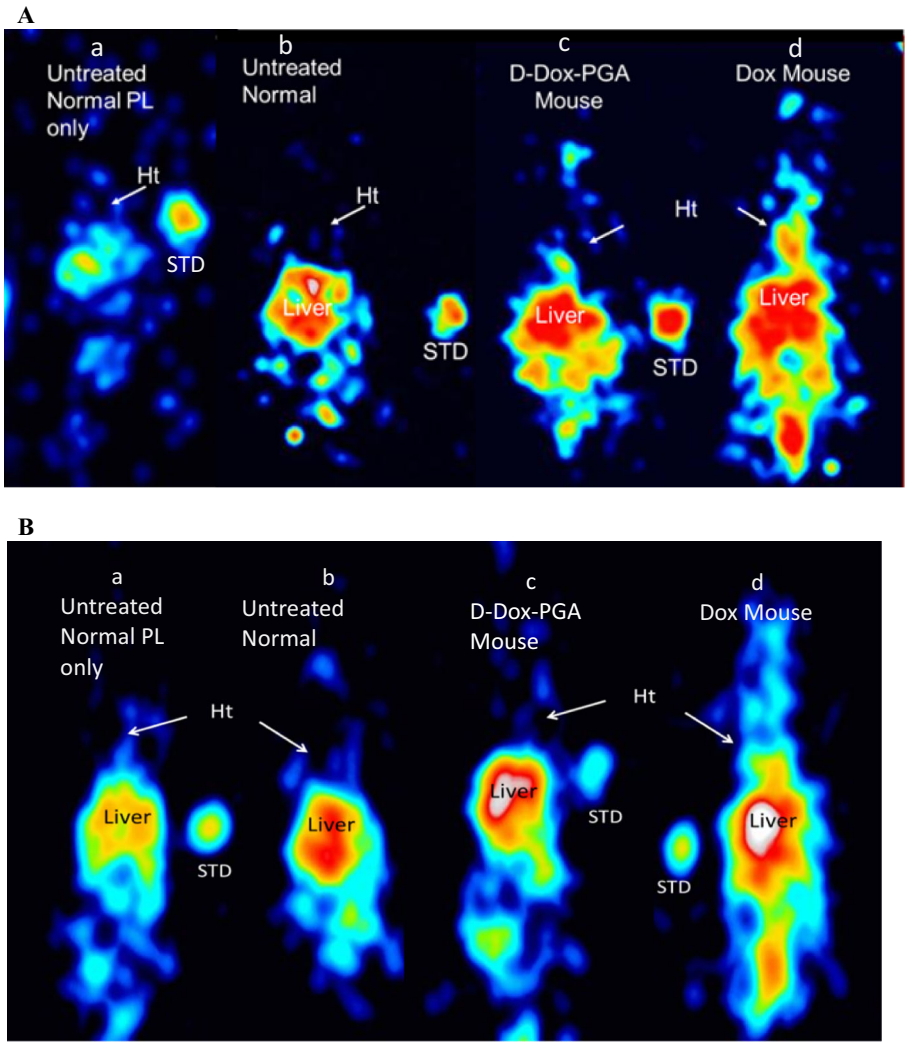
A
a
Untreated
Normal PL
only
b
Untreated
Normal
c
D-Dox-PGA
Mouse
d
Dox Mouse
Ht
STD
Liver
B
a
Untreated
Normal PL
only
b
Untreated
Normal
c
D-Dox-PGA
Mouse
d
Dox Mouse
Ht
Liver
STD
C
%ID/gm
0
1
2
3
4
Dox+BiAb+D-PL-Tc99
D-PGA-Dox+BiAb+D-PL-Tc99
BiAb+D-PL-Tc99
D-PL-Tc99
Heart
Lung
Liver
Blood
Kidney
Spleen
Stomach
Intestine
Muscle
Salivary Glands
Site of Injection

◀ **Figure 8. A**, **B** Two sets of posteroanterior gamma images of mice at 24 hours after radiotracer administration. a. Top and bottom (left) panels represent untreated control mice injected with Tc-99m DSPL alone. b. Top and bottom panels represent untreated control mice pretargeted with bsAb and targeting with Tc-99m DSPL. c. Top and bottom panels are images of mice injected with 30 mg/kg Dox-equivalent D-Dox-PGA at 39 days of the study after pretargeting with bsAb and targeting with Tc-99m DSPL. d. Top and bottom panels are images of mice injected with a single 10 mg/kg dose of Dox at 8 days post-Dox administration that are pretargeted with bsAb and targeted with Tc-99m DSPL. *Ht*, heart; *STD*, standards. **C** Biodistribution data after imaging of all mice at 24 hours. Solid bars = Dox treatment, hatch lines slanting down to the right = D-Dox-PGA treatment, horizontal hatch lines = untreated saline controls injected with bsAb and Tc-99m DSPL and hatch lines slanting down to the left = untreated controls injected with Tc-99m DSPL. Bispecific anti-myosin-anti-DTPA antibody -localized Tc-99m radioactivity is statistically significantly higher in the hearts of mice treated with one dose of Dox relative to three doses of Dox equivalent in D-Dox-PGA and in the two control groups ($P < .001$), whereas no significant differences were observed in the last three groups. (One-way ANOVA comparison).

of D-Dox-PGA in vivo due to our experimental protocol restrictions. Therefore, determination of IC_{50} of D-Dox-PGA in vivo must await additional investigation.

CONCLUSIONS

Small experimental myocardial lesions induced by Dox cardiotoxicity may be visualized by planar gamma imaged in vivo as early as 3-hour post-administration of Tc-99m-labeled polymers in the murine model. This approach may also be used to assess reduction of Dox-induced cardiotoxicity using D-Dox-PGA. Combined with our previous report of therapeutic equivalency between free Dox and D-Dox-PGA-targeted to HER-2 positive breast cancer with bispecific anti-HER-2 affibody-anti-DTPA Fab complexes,[31] and the current demonstration of reduction of cardiotoxicity with D-Dox-PGA, therapeutic efficacy may be enhanced using targeted PDC. Concurrent in vivo assessment of cardiotoxicity during chemotherapy with bsAb pretargeting

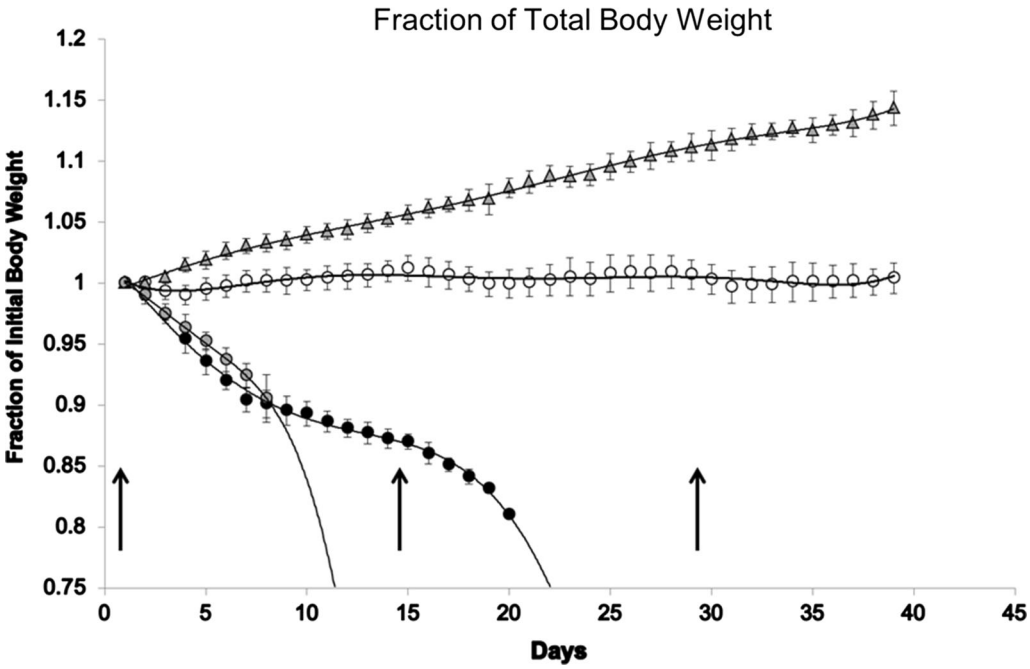

Figure 9. Relationship between fraction of the initial total body weight (*Y*-axis) and days from initiation of study (*X*-axis) in mice treated with 2 × 10 mg/kg free Dox (closed circles, $y = -3E\text{-}06x_4 + 8E\text{-}05x_3 + 0.0002x_2 - 0.0205x + 1.026$, $R^2 = 0.9954$), 1 × 10 mg/kg free Dox (gray circles, $y = 7E\text{-}10 \times 6 - 7E\text{-}08x_5 + 2E\text{-}06x_4 - 3E\text{-}05x_3 + 3E\text{-}05x_2 + 0.006x + 0.991$, $R^2 = 0.9979$), D-Dox-PGA after 3 × 10 mg/kg Dox equivalent (open circles, $y = 2E\text{-}09x_6 - 2E\text{-}07x_5 + 1E\text{-}05x_4 - 0.0003x_3 + 0.0029x_2 - 0.0123x + 1.0116$, $R^2 = 0.6076$) and untreated saline controls (gray triangles, $y = -5E\text{-}05x_4 + 0.0007x_3 - 0.0041x_2 - 0.0032x + 1.0069$, $R^2 = 0.9993$). Arrows denote day of injection of 10 mg/kg Dox or Dox equivalent.

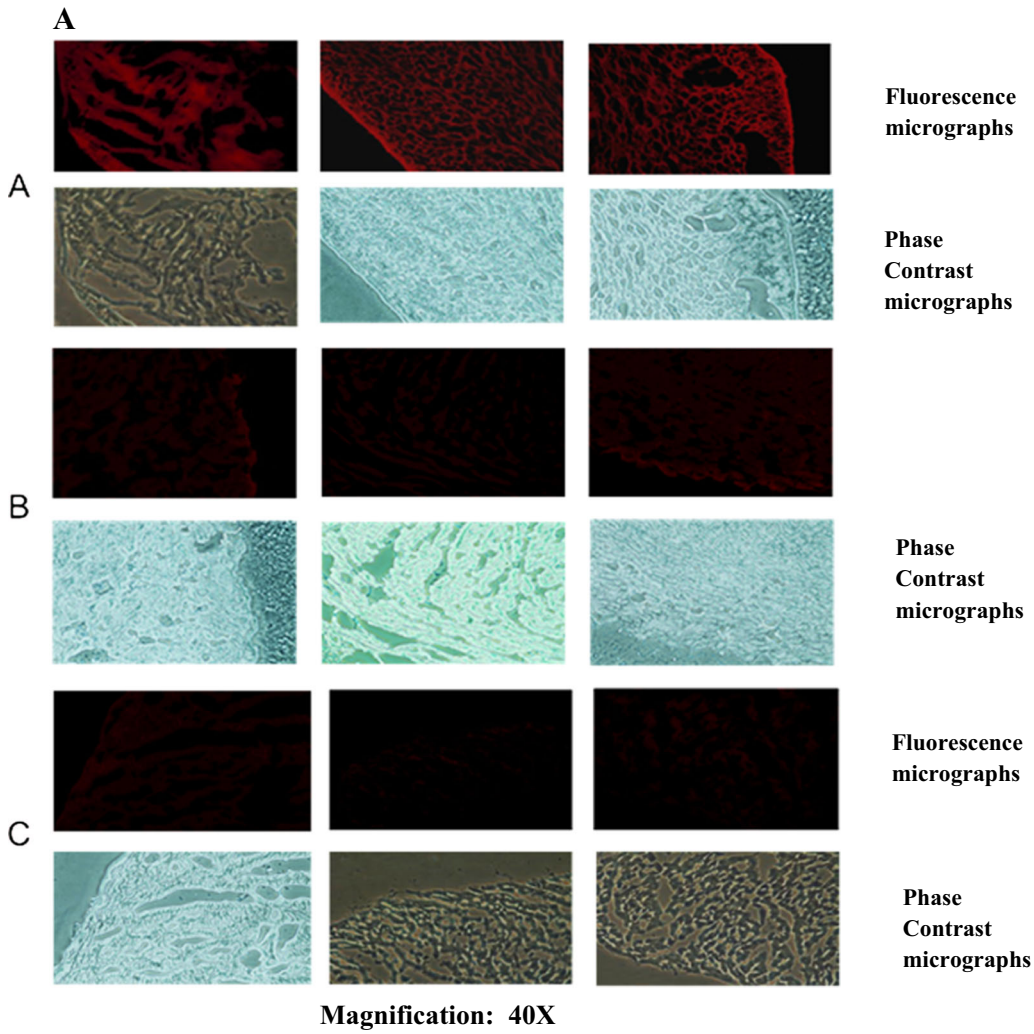

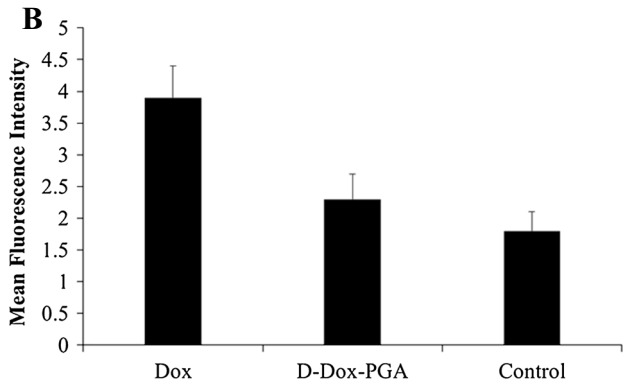

Figure 10. **A** Red (Dox) epifluorescent and phase contrast micrographs of frozen myocardial tissue sections of mice ($n = 3$) injected with Dox (a), D-Dox-PGA (b), and untreated control (c). Magnification = 40×. **B** Mean fluorescent intensity of Dox fluorescence of tissues samples described in (**A**).

and targeting with radiolabeled polymers may provide an enhanced companion-diagnostic modality.

Acknowledgements

The prototype gamma camera was provided by Andrew Weisenberger from the Jefferson National Acclerator Faciities.

Disclosure

B.A. Khaw is a co-founder of Akrivis Technologies LLC. There is no conflict of interest with regards to the work of this research for any of the authors (Rajiv Panwar, Prashant Bhattarai, Vishwesh Patil, Keyur Gada, Stan Majewski, and Ban An Khaw).

References

1. Tan C, Tasaka H, Yu KP, Murphy ML, Karnofsky DA. Daunomycin, an antitumor antibiotic, in the treatment of neoplastic disease. Clinical evaluation with special reference to childhood leukemia. Cancer 1967;20:333-53.
2. Hale JP, Lewis IJ. Anthracyclines; cardiotoxicity and its prevention. Arch Dis Child 1994;71:457-62.
3. Mallison J, Sister W, Hey H. Cardiotoxicity associated with doxorubicin. Cancer Nurs Pract 2003;2:30-4.
4. Von Hoff DD, Rozencweig M, Piccart M. The cardiotoxicity of anticancer agents. Semin Oncol 1982;9:23-33.
5. Shan K, Michael LA, Young JB. Anthracycline-induced cardiotoxicity. Ann Intern Med 1996;125:47-58.
6. Doroshow JH. Effect of anthracycline antibiotics on oxygen radical formation in rat heart. Cancer Res 1983;43:460-72.
7. Ichikawa Y, Ghanefar M, Bayeva M, WuR Khechaduri K, Prasad SVN, et al. Cardiotoxicity of doxorubicin is mediated through mitochondrial iron accumulation. J Clin Investig 2014;124:617-30.
8. Hasinoff BB, Herman EH. Dexrazoxane: how it works in cardiac and tumor cells. Is it a prodrug or is it a drug? Cardiovasc Toxicol 2007;2:140-4.
9. Swain SM, Vici P. The current and future role of dexrazoxane as a cardioprotectant in anthracycline treatment: expert panel review. J Cancer Res Clin Oncol 2004;130:1-7.
10. Zhang S, Liu X, Bawa-Khalfe T, Lu LS, Lyu YL, Liu LF, et al. Identification of the molecular basis of doxorubicin-induced cardiotoxicity. Nat Med 2012;18:1639-42.
11. Bellingham M, Bristow M. Evaluation of anthracycline cardiotoxicity: predictive ability and functional correlation of endomyocardial biopsy. Cancer Treat Symp 1984;3:71-6.
12. Vejpongsa P, Yeh ETH. Prevention of anthracycline-induced cardiotoxicity. J Am Col Cardiol 2014;64:938-45.
13. Schwartz RG, Jain D, Storozynsky E. Traditional and novel methods to assess and prevent chemotherapy-related cardiac dysfunction noninvasively. J Nucl Cardiol 2013;20:443-64.
14. Florescu M, Cinteza M, Vinereanu D. Chemotherapy-induced cardiotoxicity. Maeduca J Clin Med 2013;8:59-67.
15. Bennink RJ, van den Hoff MJ, van Hemert FJ, de Brun KM, Spijkereboer AL, van den Vanderheyden J, et al. Annexin V imaging of acute doxorubicin cardiotoxicity (apoptosis) in rats. J Nucl Med 2004;45:842-8.
16. Estorch M, Carrio I, Berna L, Mertinez-Duncker C, Alonso C, Germa JR, et al. Indium-111-antimyosin scintigraphy after doxorubicin therapy in patients with advanced breast cancer. J Nucl Med 1990;31:1965-9.
17. Carrio I, Lopez-Pousa A, Estorch M, Duncker C, Berna L, Torres G, et al. Detection of doxorubicin cardiotoxicity in patients with sarcomas by indium-111-antimyosin monoclonal antibody studies. J Nucl Med 1993;34:1503-7.
18. Valdés Olmos RA, ten Bokkel Huinink WW, ten Hoeve RF, Van Tinteren H, Bruning PF, Van Vlies B, et al. Usefulness of indium-111 antimyosin scintigraphy in confirming myocardial injury in patients with anthracycline-associated left ventricular dysfunction. Ann Oncol 1994;5:617-22.
19. Yasuda T, Palacios IF, Dec WG, Fallon JT, Gold H, Leinbach RC, et al. Indium 111-monoclonal antimyosin antibody imaging in the diagnosis of acute myocarditis. Circulation 1978;76:306-11.
20. Carrio I, Berna L, Ballester M, Estorch M, Obrador D, Cladellas M, et al. Indium-111 antimyosin scintigraphy to assess myocardial damage in patients with suspected myocarditis and cardiac rejection. J Nucl Med 1988;29:1893-900.
21. Peker C, Sarda-Mantel L, Loiseau P, Rouzet F, Nazneen L, Martet G, et al. Imaging apoptosis with Tc-99m-annexin-V in experiment subacute myocarditis. J Nucl Med 2004;5:1081-6.
22. Kopecek J. Polymer-drug conjugates: origins, progress to date and future directions. Adv Drug Deliv 2013;65:49-59.
23. Li C, Wallace S. Polymer-drug conjugates: recent development in clinical oncology. Adv Drug Deliv Rev 2008;60:886-98.
24. Khaw BA, Tekabe Y, Johnson LL. Imaging experimental atherosclerotic lesions in ApoE knockout mice: enhanced targeting with Z2D3-anti-DTPA BISPECIfiC ANTIBODY and 99m Tc-labeled negatively charged polymers. J Nucl Med 2006;47:868-76.
25. Gada K, Patil V, Panwar P, Majewski S, Tekabe Y, Khaw BA. Pretargeted gamma imaging of murine metastatic melanoma lung lesions with bispecific antibody and radiolabeled polymer drug conjugates. Nucl Med Commun 2011;32:1231-40.
26. Khaw BA, Petrov A, Narula J. Complementary roles of antibody affinity and specificity for in vivo diagnostic cardiovascular targeting: How specific is antimyosin for irreversible myocardial damage? J Nucl Cardiol 1999;6:316-23.
27. Habeeb AF. Determination of free amino groups in proteins by trinitrobenzenesulfonic acid. Anal Biochem 1966;14:328-36.
28. Khaw BA, Gold HK, Yasuda T, Leinbach RC, Kanke M, Fallon JT, et al. Scintigraphic quantification of myocardial necrosis in patients after intravenous injection of myosin specific antibody. Circulation 1986;74:501-8.
29. Patil V, Gada K, Panwar R, Varvarigou A, Majewski S, Weisenberger A, et al. Imaging small human prostate cancer xenografts after pretargeting with bispecific bombesin-antibody complexes and targeting with high specific radioactivity labeled polymer-drug-conjugates. EJNMMI 2012;39:824-39.
30. Sun MM, Beam KS, Cerveny CG, Hamblett KJ, Blackmore RS, Torgov MY, et al. Reduction-alkylation strategies for the modification of specific monoclonal antibody disulfides. Bioconjug Chem 2005;16:1282-90.
31. Khaw BA, Gada KS, Patil V, Panwar R, Mandapati S, Hatefi A, et al. Bispecific antibody complex pre-targeting and targeted delivery of polymer-drug-conjugates for imaging and therapy in dual-human mammary cancer xenografts. EJNMMI. 2014;41:1603. https://doi.org/10.1007/s00259-014-2738-2.
32. Gada KS, Patil V, Panwar R, Hatefi A, Khaw BA. Bispecific antibody complex pretargeted delivery of polymer-drug-conjugates for cancer. Drug Deliv Trans Res 2012;2:65-76.
33. Patil V, Gada K, Panwar R, Majewski S, Tekabe Y, Varvarigou A, et al. In vitro demonstration of enhanced prostate cancer toxicity: pretargeting with bombesin bispecific complexes and targeting with polymer-drug-conjugates. J Drug Target 2013;21:1012-21.

34. Arnold RD, Slack JE, Straubinger RM. Quantification of Doxorubicin and metabolites in rat plasma and small volume tissue samples by liquid chromatography/electrospray tandem mass spectroscopy. J Chromatogr B 2004;808:141-52.
35. Hammond W, Tekabe Y, Johnson L, Majewski S, Popov V, Kross B, et al. Development of high performance mini gamma cameras based on LaBr3scintillator and H8500 and H9500 PSPMTs and their use in small animal studies. Medical Imaging Conference. 2006.
36. Bhattarai P, Vance D, Hetafi A, Khaw BA. An in vitro demonstration of overcoming drug resistance in SKOV3 TR and MCF7 ADR with targeted delivery of polymer pro-drug conjugates. J Drug Target 2017;25:436-50.
37. Singal P, Iliskovic N, Li T, Kumar D. Adriamycin cardiomyopathy: pathophysiology and prevention. FASEB J 1997;11:931-6.
38. Chatterjee K, Zhang J, Honbo N, Karliner JS. Doxorubicin cardiomyopathy. Cardiology 2010;115:155-62.
39. Granger CB. Prediction and prevention of chemotherapy-induced cardiomyopathy: can it be done? Circulation 2006;114:2432-3.
40. Lipshultz SE, Adams MJ. Cardiotoxicity after childhood cancer: beginning with the end in mind. J Clin Oncol 2010;28:1276-81.
41. Lorusso D, Di Stefano A, Carone V, Fagotti A, Pisconti S, Scambia G. Pegylated liposomal doxorubicin-related palmar-plantar erythrodysesthesia ('hand-foot' syndrome). Ann Oncol 2007;18:1159-64.
42. Yuan Y, Orlow SJ, Curtin J, Downey A, Muggia F. Pegylated liposomal doxorubicin (PLD): enhanced skin toxicity in areas of vitiligo. Case report. Ecancermedicalscience. 2008;2:111.
43. Levine AM, Tulpule A, Espina B, Sherrod A, Boswell WD, Lieberman RD, et al. Liposome encapsulated doxorubicin in combination with standard agents cyclophosphamide, vincristine, prednisone) in patients with newly diagnosed AIDS-related non-Hodgkin's lymphoma: results of therapy and correlates of response. J Clin Oncol 2004;22:2662-70.
44. U.S. Food and Drug Administration. Drug Safety and Availability. FDA statement on dexrazoxane. July 20, 2011. http://www.fda.gov/Drugs/DrugSafety/ucm263729.htm.
45. Lipshultz SE, Rifai N, Dalton VM, Levy DE, Silverman LB, Lipsitz SR, et al. The effect of dexrazoxane on myocardial injury in doxorubicin treated children with acute lymphoblastic leukemia. N Engl J Med 2004;351:145-53.
46. Swain SM, Whaley FS, Gerber MC, Weisberg S, York M, Spicer D, et al. Cardioprotection with dexrazoxane for doxorubicin-containing therapy in advanced breast cancer. J Oncol 1997;15:1318-32.
47. Cai C, Lothstein L, Morrison RR, Hofmann PA. Protection from doxorubicin-induced cardiomyopathy using the modified anthracycline N-benzyladriamycin 14-valerate (AD 198). J Pharmacol Exp Ther 2010;335:223-30.
48. Hall TS, Baumgartner WA, Borkon AM, LaFrance ND, Traill TA, Norris S, et al. Diagnosis of acute cardiac rejection with anti-myosin monoclonal antibody, phosphorous nuclear magnetic resonance imaging, two-dimensional echocardiography, and endocardial biopsy. J Heart Transplant 1986;5:419-24.
49. Vora J, Khaw BA, Narula J, Boroujerdi M. Protective effect of butylated hydroxyanisole on Adriamycin induced cardiotoxicity. J Pharm Pharmacol 1996;48:940-4.
50. Hiroe M, Otha Y, Fujita N, Nagata M, Toyozaki T, Kusakabe K, Sekiguchi M, Marumo F. Myocardial uptake of ^{111}In monoclonal antimyosin Fab in detecting doxorubicin cardiotoxicity in rats. Circulation 1992;86:1965-72.
51. Su H, Gorodny N, Gomez LP, Gangadharmath U, Mu F, Chen G, Walsh JC, Szardenings K, Kolb HC, Tamarappoo B. Noninvasive molecular imaging of apoptosis in a mouse model of anthracycline-induced cardiotoxicity. Circ Cardiovasc Imaging. 2015;8:e001952. https://doi.org/10.1161/circimaging.114.001952.
52. Van Decker WA. Imaging and chemotherapy cardiotoxicity: a long-playing story still seeking precision and improved outcome/management data. J Nucl Cardiol 2016;23:98-100.
53. Narula J, Strauss HW, Khaw BA. Antimyosin positivity in doxorubicin cardiotoxicity: earlier than the conventional evidence. J Nucl Med 1993;34:1507-9.
54. de Geus-Oei LF, Mavinkurve-Giroothuis AMC, Bellersen L, Gotthardt M, Oyen WJG, Kapusta L, van Laarhoven HWM. Scintigraphic techniques for early detection of cancer-induced cardiotoxicity. J Nucl Med 2011;52:560-71.